

Reconstruction of the turbulence density fluctuation profile from reflectometry phase fluctuation measurements revisited

M. Schubert¹, A. Popov², S. Heuraux¹, E. Gusakov² and T. Gerbaud³

¹ LPMIA UMR 7040, UHP Nancy I, BP 239, 54506 Vandoeuvre Cedex, France

² Ioffe Institute, Politekhnicheskaya 26, 194021 St.Petersburg, Russia

³ Association EURATOM/CEA, CEA/DSM/IRFM, CEA-Cadarache, 13108 St Paul-lez-Durance, France

1 Introduction

Progress in understanding phenomena like anomalous transport or ELMs requires plasma turbulence diagnostics with high spatial and temporal accuracy. For the plasma density the variance σ^2 of phase fluctuations in microwave reflectometry is frequently used [1, 2] to determine the absolute value of the fluctuation level $\langle \delta n^2 \rangle$ located at the O-mode cut-off:

$$\sigma^2 = \pi \frac{k_0^2 L}{k_{\text{eff}}} \frac{\langle \delta n^2 \rangle}{n_{\text{cut-off}}^2}. \quad (1)$$

This relation is exact in a linear density profile with a gradient length L and a homogeneous fluctuation level $\langle \delta n^2 \rangle = \text{const}$, and assuming that the Born approximation is valid [3]. Analytical formulae exist for the effective fluctuation wavenumber k_{eff} in a given radial wavenumber spectrum [4]. In this paper we verify the formulae for a Gaussian and for a Tore Supra like exponential spectrum [5] in a full scale comparison with the results of a 1D Full-Wave code.

Replacing L with the local gradient length at the cut-off, equation (1) can also be a good approximation for inhomogeneous profiles of density and fluctuation level. Generally it fails in a negative gradient of the fluctuation level along the line-of-sight [6]. In such case we suggest the 1D equation (2) where the weighting function G is introduced.

$$\sigma^2 = \pi k_0^2 L \int_{x_{\text{edge}}}^{x_c} G(x) \frac{\langle \delta n^2(x) \rangle}{n_{\text{cut-off}}^2} dx \quad (2)$$

G depends on the average density profile and it usually has a maximum at the cut-off (position $x = x_c$). We discuss G for a Gaussian wavenumber spectrum, again verifying the results with a Full-Wave simulation. Finally we test an inversion algorithm to deduce the profile of the fluctuation level from σ^2 measured at different frequencies.

2 Analytical formulae

The derivation of the following equations from first principles is published elsewhere [4]. The theory is for O-mode with a cut-off density $n_{\text{cut-off}} = m_e \epsilon_0 c_0^2 k_0^2 e^{-2}$ and a local index of refraction $N(x) = k(x)/k_0 = \sqrt{1 - n_e(x)/n_{\text{cut-off}}}$. It is assumed that the system size L is large compared to typical correlation lengths l_c in the turbulence, so that the plasma density fluctuations can be modelled in wavenumber space with a fixed amplitude spectrum and random phases. Furthermore $|\langle \delta n \rangle / n_{\text{cut-off}}| \ll l_c/L$ in order

to avoid secondary cut-offs, and $l_c \gg (L/k_0^2)^{1/3}$ to neglect backscattering far from the cut-off. Finally, in a linear density gradient and homogeneous fluctuation level σ^2 can be expressed as an integral in wavenumber space [4]:

$$\sigma^2 \sim \frac{k_0^2 L}{n_{\text{cut-off}}^2} \int \frac{\delta n_\kappa^2}{|\kappa|} \left| F(\sqrt{\kappa}L) \right|^2 d\kappa, \quad \text{where} \quad F(s) = \int_0^s \exp(i\zeta^2) d\zeta.$$

An accurate evaluation yields the effective fluctuation wavenumber k_{eff} for equation (1), where $l_c \approx 4\rho_i$ for the Tore Supra case, ρ_i = ion Larmor radius, and $\gamma \approx 0.577$.

$$\text{Gaussian: } \delta n_\kappa^2 \sim \exp[-l_c^2 \kappa^2/4] \rightarrow k_{\text{eff}}^{(G)} = \frac{\sqrt{\pi}}{l_c} \left(\ln \left[\frac{8L}{\pi l_c} \right] - \frac{\gamma}{2} + 1 \right)^{-1} \quad (3)$$

$$\text{Tore Supra [5]: } \delta n_\kappa^2 \sim \exp[-4\rho_i \kappa] \rightarrow k_{\text{eff}}^{(H)} = (4\rho_i)^{-1} \left(\ln \left[\frac{L}{4\rho_i} \right] + 2 \ln 2 \right)^{-1} \quad (4)$$

In a more general approach [4] equation (2) can be derived for a Gaussian wavenumber spectrum. It is, however, necessary that the characteristic length of the turbulence inhomogeneity $\langle \delta n^2(x) \rangle$ is larger than l_c , but still small compared to the system size. The solution in a linear density gradient is displayed in equation (5), where $I_0(s)$ is the modified Bessel function. In an arbitrary density profile this can be used for the near distance to the cut-off. More far away the solution has the asymptotic displayed in equation (6), which takes into account arbitrary density profiles via the index of refraction $N(x)$.

$$G_{\text{near}}(x) = \exp \left[-\frac{(x-x_c)^2}{2l_c^2} \right] I_0 \left[\frac{(x-x_c)^2}{2l_c^2} \right] \quad (5) \quad G_{\text{far}}(x) = \frac{l_c}{\sqrt{\pi}LN^2(x)}. \quad (6)$$

3 Numerical setup

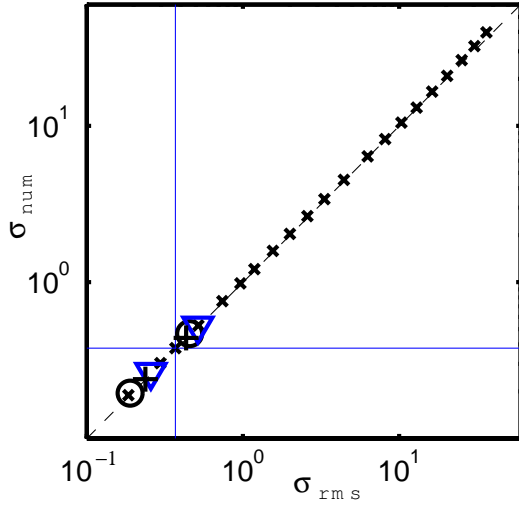
The plasma density is modelled as superposition of an average profile and a fluctuating part: $n_e = \bar{n}(x) + \delta n(x, t)$. We assume that the turbulence can be represented as a random superposition of modes $\delta n(x, t) = \sum \delta n_\kappa \times \cos[\kappa x + \varphi_t(\kappa)]$ where the mode phase spectra $\varphi_t(\kappa)$ are random numbers $\in [0 \dots 2\pi]$. The summation is implemented using the discrete Fourier transform. Since the average value is defined by $\bar{n}(x)$, we set $\delta n_0(\kappa = 0) = 0$. We note that turbulent modes with long wavelengths are more effective in contributing to σ^2 and, therefore, the wavenumber of the longest mode in the system must be at least $60 \times L$ in order to achieve convergence within 1% of the final value (continuous spectrum). Inhomogeneous turbulence is generated by multiplying $\delta n(x, t)$ with an envelope function. Characteristic lengths of the envelope are large compared to l_c , thus we neglect the impact of the envelope on the spectrum.

In order to simulate the reflectometry measurement, the Helmholtz equation for the electric field of the launched microwave is solved in the cold plasma approximation, using a 4th order Numerov scheme [3]. The phase variance σ^2 is obtained by evaluating the measurement in a significant number (~ 200000) of instances t of the turbulence.

4 Comparison: Full-Wave code vs analytical formula

We compare the analytical solution with the result $\sigma_{\text{num}} = \sqrt{\sigma^2}$ obtained numerically in a linear density gradient and homogeneous turbulence. For a Gaussian spectrum (Eqs. 1+3)

the result is displayed in Fig. 1. All parameter dependencies are in good agreement. If the relative fluctuation level $> 4\%$ then non linear backscattering becomes important and the numerical result is systematically higher than the analytical one. A similar comparison



has been carried out for the Tore Supra like spectrum from equation (4).

Figure 1: $\sqrt{\sigma^2}$ from Full-Wave simulations as a function of the analytical solution for a Gaussian spectrum. Cross-hair: starting point for parameter scans: $L = 58$ cm, 47 GHz, $l_c = 3$ cm, $\langle \delta n_{\text{rms}} \rangle / n_{\text{cut-off}} = 0.001$.

x symbols: $\langle \delta n_{\text{rms}} \rangle / n_{\text{cut-off}} = 5 \cdot 10^{-4} \dots 0.1$
Open circles: $f = 24$ GHz, 58 GHz. + signs: $l_c = 1$ cm, 4.5 cm. Blue triangles: $L = 32.1$ cm, 100 cm. The dashed line indicates identical values on the two coordinates.

5 Arbitrary profiles of density and fluctuation level

Profiles of density and fluctuation level are set up similarly to those in Tore Supra (Fig. 2). Two different models are used for the density profile: Model A (concave) approximates the plasma edge very well, and model C (convex) is more accurate in the plasma core.

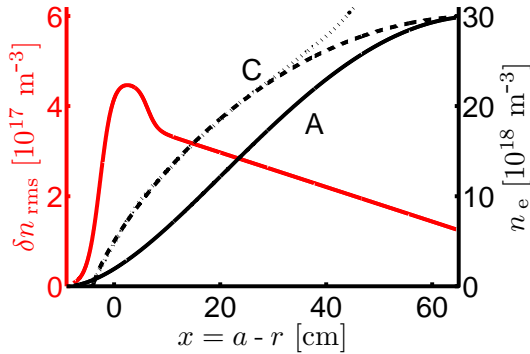
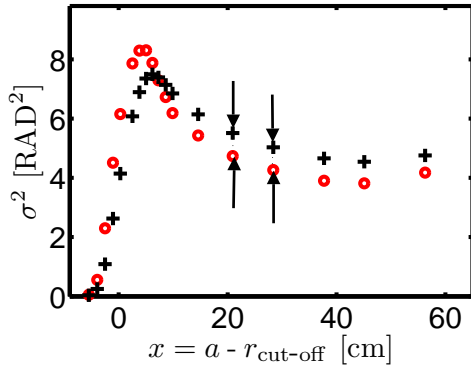


Figure 2: Input profiles for the Full-Wave simulation. Red: model for the fluctuation level $\delta n_{\text{rms}} = \sqrt{\langle \delta n^2 \rangle}$ based on data from Tore Supra # 38316. Black: density profile models A (concave) and C (convex). Dotted line: profile measured in Tore Supra # 38316. r : radial profile coordinate. a : radius of the plasma boundary.

We use the Full-Wave code in order to simulate a measurement, producing a set of σ^2 at 18 different frequencies between 5.5 and 48 GHz, cf. Fig. 3. From this set we directly evaluate a first estimate $\langle \delta n^2(x) \rangle$ by means of equation 3 (Gaussian spectrum!). In the case of model C the first estimate reproduces the input fluctuation profile very well, while for model A there are deviations, displayed in Fig. 4.

To improve the situation for model A, we reconstruct the σ^2 data from the first estimate $\langle \delta n^2(x) \rangle$, but this time using the more accurate formula (2) for each frequency. The numerical integration is carried out in a continuous profile which is created by linear interpolation (Fig. 4). The weighting function for a given frequency and cut-off position x_c is: $G = G_{\text{near}}$ (Eq. 5), if $x - x_c \leq 3l_c$, and $G = G_{\text{far}}$ (Eq. 6), if $x - x_c > 3l_c$. It is displayed with arrows in Fig. 3 that the reconstructed σ^2 data differ from the input. Hence we apply an optimisation algorithm in order to minimize this deviation. The algorithm processes

pairs of σ^2 and δn_{rms} samples, starting at the plasma edge, and varying the δn_{rms} value until the deviation in σ^2 vanishes. The obtained result reproduces the input much better,



see Fig. 4.

Figure 3: Red circles: Phase variances from Full-Wave simulations. Input density profile A from Fig. 2. Horizontal axis: cut-off locations of the launched microwave frequencies. Black crosses: phase variances reconstructed from the first estimate of the fluctuation level profile (black crosses in Fig. 4) using equation (2).

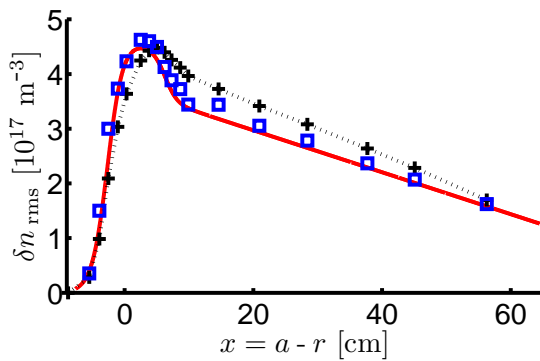


Figure 4: Black crosses: fluctuation level deduced from the σ^2 data of Fig. 3 using Eqs. (1) and (3). The linear interpolation is overplotted using a dotted line, and $\delta n_{\text{rms}} = 0$ was introduced artificially at the edge on the left. Blue square symbols: Result of the optimisation algorithm that uses Eq. (2). The input profile is displayed with solid red line for comparison.

6 Discussion and Conclusions

Analytical expressions for the phase fluctuations in O-mode reflectometry have been tested. In general they are valid for relative fluctuation levels $< 4\%$. Comparing with Full-Wave code results we show that the accuracy depends on the shape of the background density profile, it is in particular good in the case of a convex profile. This is due to the scaling of the phase fluctuations with the local gradient length. For more difficult cases we successfully tested a simple inversion algorithm.

7 Acknowledgements

Financial support by RFBR grants 06-02-17212, 07-02-92162-CNRS, and ANR grant FI-071215-01-01 is acknowledged.

8 Bibliography

- [1] A. Krämer-Flecken et al., Physical Review Letters **97** (2006) 045006.
- [2] R. Sabot et al., Plasma Phys. Controlled Fusion **48** (2006) B421.
- [3] C. Fanack et al., Plasma Phys. Controlled Fusion **38** (1996) 1915.
- [4] E. Gusakov and A. Popov, Plasma Phys. Controlled Fusion **44** (2002) 2327.
- [5] P. Hennequin et al., Plasma Phys. Controlled Fusion **46** (2004) B121.
- [6] M. Schubert et al., *34th EPS Conf. Plasma Phys. (Warsaw)*, ECA **31F** (2007) P5.090.